Received: 18 May 2021 | Revised: 29 July 2021 | Accepted: 3 August 2021

DOI: 10.1002/aoc.6413

RESEARCH ARTICLE

Applied Organometallic Chemistry WILEY

Functionalized nanomagnetic graphene by ion liquid containing phosphomolybdic acid for facile and fast synthesis of paracetamol and aspirin

Elahe Nasiri[1] | **Feridoon Kooshki**[1] | **Mohammad Kooti**[1] | **Rezvan Rezaeinasab**[2]

[1]Department of Chemistry, Shahid Chamran University of Ahvaz, Ahvaz, Iran

[2]Department of Medicinal Chemistry, School of Pharmacy, Lorestan University of Medical Sciences, Khorramabad, Iran

Correspondence
Mohammad Kooti and Elahe Nasirii, Department of Chemistry, Shahid Chamran University of Ahvaz, Ahvaz, Iran.
Email: m_kooti@scu.ac.ir; elahe_mahz84@yahoo.com

Funding information
Research Council of Shahid Chamran University of Ahvaz, Iran, Grant/Award Number: 1398

A nanocomposite has been synthesized by supporting of polyaniline-modified polyoxometalate-paired poly(ionic liquid) on the surface of magnetic graphene and characterized by various techniques. The fabricated nanocomposite was found to be a versatile catalyst for the synthesis of paracetamol and aspirin drugs showing high activity and selectivity. The observed high catalytic activity of the newly synthesized catalyst, in the preparation of these two important drugs, can be attributed to the presence of graphene, which provides high surface area for the supporting of polyaniline–polyoxometalate pair and also to the strong acidity of the solid acid. This catalytic system has several advantages, such as simple experimental process, easy separation of the product, solvent-free condition, efficient isolation, and recovery of the magnetic catalyst as well as high reusability.

KEYWORDS
aspirin, ionic liquid, magnetic graphene, nanocatalyst, paracetamol

1 | INTRODUCTION

Paracetamol and aspirin are produced in massive scales annually because of their widespread use in medicine as antipyretic and analgesic drugs. In addition to their use as drugs, aspirin (acetylsalicylic acid) and paracetamol (*N*-(4-hydroxyphenyl)acetamide) are also employed as precursors for the synthesis of several valuable organic and pharmaceutical materials. Therefore, the synthesis methods for paracetamol and aspirin should be highly efficient, simple, safe, and cost effective to be suitable for high-scale production.[1–5] Concentrated sulfuric and phosphoric acids are most frequently used as catalysts for the preparation of these drugs. However, the mentioned acids are highly corrosive, and the obtained yield of the drugs is rather poor.[6–10]

Solid inorganic acids are another alternative commonly used as catalysts toward various organic reactions. In this regard, Keggin-type heteropolyacids and other derivatives have been reported to be efficient catalysts for the synthesis of organic compounds. These solid acids have been used as catalysts either in a free state or supported on proper substrates. Among the various heteropolyacids, phosphomolybdic acid (PMoA), as Brønsted acid catalyst, has attracted much attention.[11–20]

On the other hand, polyaniline (PANI), one of the well-known conductive polymers, is widely used as support for the designing of various hybrid composites. This is due to its interesting properties, such as low weight, ease of synthesis, low cost, flexibility, environmental stability, and optical and characteristic redox properties. Therefore, Zhang et al. have supported molybdic acid (H_2MoO_4, MoA) on PANI microstructure through its Mo–OH groups. The obtained MoA–PANI hybrid is of some interest in biochemical and catalysis research because the presence of protons in the structure of PANI

provides acidic sites and the Mo(IV) center exhibits remarkable coordination chemistry.[21]

The magnetic nanocatalysts, as heterogeneous catalysts with high surface area and consequently more catalytic sites, can efficiently interact with the precursors present in the reaction mixture. They can also be readily separated from the reaction media and recycled and thus have the advantages of both heterogeneous and homogeneous catalysts. Efficient separation of these types of catalysts is achieved by merely applying an external magnetic field. Therefore, magnetic nanocatalysts can be considered as green catalysts and are expected to be superior to nonmagnetic heterogeneous or homogeneous counterparts.[22–34]

Although several methods have been so far reported for the synthesis of paracetamol and aspirin, finding highly efficient and more environmentally friendly methods for the preparation of these important drugs is still of great value. Therefore, in this study, we have fabricated a magnetic hybrid, composed of magnetic graphene, PANI, and PMoA, through a straightforward process. In this procedure, nanoscale graphene plates were first magnetized by depositing of manganese ferrite (MF) nanoparticles on their surfaces. This was then followed by coating of the magnetic graphene plates with PANI and subsequently functionalizing with PMoA. Each of the components in the prepared hybrid, designated as G/MF@PANI-PMoA, has its own advantage. That is, graphene will provide higher surface area, MF ensures the magnetic property, and PANI offers means for the anchoring of PMoA, the Brønsted acid, on the core of this hybrid. The catalytic activity of this magnetic nanocomposite was examined for the synthesis of paracetamol and aspirin under solvent-free condition. It was found that the synthesis of these drugs is achieved readily at mild conditions in the presence of a catalytic amount of this catalyst. Moreover, due to the magnetic and heterogeneous characters of this catalyst, it can be easily recovered from the reaction mixture and reused for several times.

2 | EXPERIMENTAL

2.1 | Chemicals

Aniline (Sigma-Aldrich) was first distilled under vacuum prior to use. PMoA was prepared as reported.[35] The final products of the catalytic reactions were characterized by comparison of their physical data, such as FT-IR and ^{1}H NMR spectra, with those of known samples. ^{1}H NMR spectra were recorded on a Bruker Advance DPX 400-MHz spectrometer using TMS as internal standard. FT-IR spectra were obtained using a FT BOMEM MB102 spectrophotometer. Powder x-ray diffraction (PXRD) patterns were taken with a Philips x-ray diffractometer (model PW1840) over a 2θ range from 10° to 80° using Cu K_α radiation ($\lambda = 1.54056$ Å). The FESEM images were obtained using a Hitachi Japan S4160 scanning electron microscope, and TEM images were taken with Philips CM10-HT 100-K instrument. The magnetic properties of the samples were studied by vibrating sample magnetometry (VSM) of Meghnatis Daghigh Kavir Company. The molybdenum content of the G/MF@PANI-PMoA nanocatalyst was determined using an ICP-AES instrument (HORIBA Jobin Yvon, Longjumeau Cedex, France). Gas chromatography (GC) experiments were performed with a Shimadzu GC-16A instrument using a 2-m column packed with silicone DC-200 or carbowax 20M.

2.2 | Preparation of G/MF@PANI-PMoA nanocomposite

Graphene/manganese ferrite (G/MF) nanocomposite was prepared using the previously reported method.[36] A 1.0 g of G/MF was added to 50 ml of aqueous solution of 0.5 M nitric acid containing 0.1 M aniline and 0.125 M ammonium peroxydisulfate. The reaction mixture was stirred for 2 h at room temperature. The resulting precipitate, consisted of G/MF and PANI, was then isolated by applying a magnet to fix it on the wall of the reaction vessel. The product (G/MF@PANI) was washed with ethanol twice and dried at 60°C for 2 h in an oven. In the next step, 1.0 g of the pre-synthesized G/MF@PANI with 0.5 g of PMoA was introduced into ethanol/water solution (at the ratio of 5:35) and stirred at room temperature for 24 h. The resulting black precipitate (G/MF@PANI-PMoA) was then separated magnetically and washed twice with distilled water and dried at 60°C in an oven for 3 h. The amount of molybdenum content in the nanocomposite was measured by ICP analysis to be 0. 360 mmol/g. The step-by-step preparation of G/MF@PANI-PMoA nanocatalyst is shown in Scheme 1.

2.3 | Synthesis of paracetamol in the presence of G/MF@PANI-PMoA

A mixture of 4-hydroxyaniline (1.0 mmol, 0.1 g), acetic anhydride (2 ml, 1.5 mmol), and G/MF@PANI-PMoA

nanocatalyst (0.1 g) was stirred at room temperature under solvent-free condition (Figure S1). The progress of the reaction was monitored by TLC technique, and it was completed in 15 min. The heterogeneous nanocatalyst was magnetically separated, washed with ethanol, and dried for reuse in a new reaction. The remaining residue was then recrystallized in deionized water to give pure paracetamol with 98% yield (Table 1).

2.4 | Preparation of aspirin catalyzed by G/MF@PANI-PMoA

A mixture of salicylic acid (1.0 mmol, 0.14 g) and acetic anhydride (2.5 ml, 3 mmol) with catalytic amount of G/MF@PANI-PMoA nanocatalyst (0.1 g) was stirred at room temperature and solvent-free conditions (Figure S2). The progress of the reaction was continuously monitored by TLC and took only 30 min for the reaction to be completed. Again, the heterogeneous nanocatalyst was isolated via applying an external magnetic field, washed with ethanol, and dried to be ready for reuse in a new reaction. Distilled water was added to the remained organic phase and placed in an ice bath. The residual acetic anhydride is converted to acetic acid and was removed from the reaction media. The crystals of aspirin were separated and dissolved in 48 ml of ethanol/water solvent, in a ratio of 3:1, at 60°C. The solution was cooled to room temperature and placed in an ice bath to reform pure aspirin crystals with 97% yield (Table 1). Identification of the products in both of these reactions was achieved by FT-IR and H^1NMR spectrometry techniques and CHN analysis.

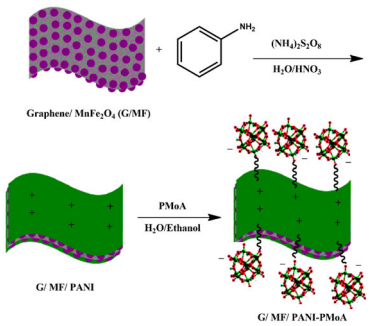

SCHEME 1 Stepwise preparation of G/MF@PANI-PMoA nanocatalyst

3 | RESULTS AND DISCUSSION

In order to characterize of the as-prepared four-component G/MF@PANI-PMoA nanocatalyst and confirming its composition, FT-IR spectroscopy and other techniques were utilized.

3.1 | FT-IR spectroscopy

The FT-IR spectra of G/MF@PANI-PMoA, $H_3PMo_{12}O_{40}$, and G/MF are depicted in Figure 1. In the FT-IR spectrum of G/MF (Figure 1c), two peaks at 463 and 582 cm^{-1} are observed, which can be assigned to Fe–O stretching in the octahedral and tetrahedral sites of $MnFe_2O_4$, respectively. The observed peak at 3438 cm^{-1} region is related to OH stretching vibrations on surface of $MnFe_2O_4$ nanoparticles. Also, the graphitic C=C stretching band at about 1560 cm^{-1} is observed. The peaks belonging to $MnFe_2O_4$, with some shift (412 and 524 cm^{-1}), are clearly seen in Figure 1a for

TABLE 1 Synthesis of paracetamol and aspirin catalyzed by G/MF@PANI-PMo

Entry	Starting material	Starting material	Product	Yield (%)	TON	TOF (h^{-1})
1	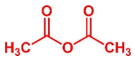	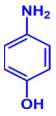	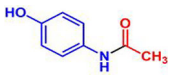	98	376.5	1470
2	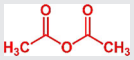	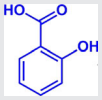	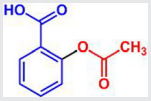	97	194	388

Abbreviations: TOF, turnover frequency = the catalytic turnover per unit time; TON, turnover number = number of moles of product formed per mole of Mo in the catalyst.[35]

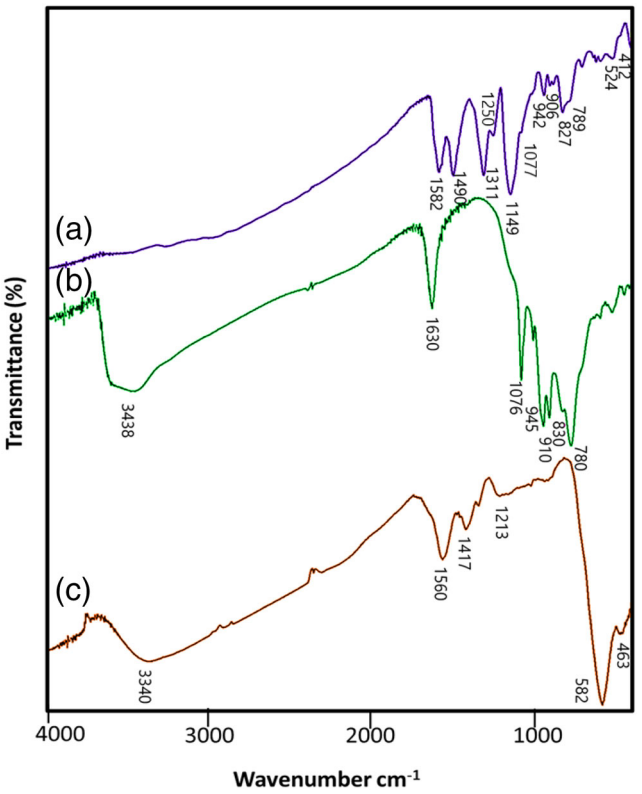

FIGURE 1 FT-IR spectra of G/MF@PANI-PMoA (a), PMoA (b), and graphene/$MnFe_2O_4$ (c)

G/MF@PANI-PMoA, indicating the presence of this magnetic spinel ferrite in the nanocomposite.

FT-IR spectrum of the prepared $H_3PMo_{12}O_{40}$ (Figure 1b) in the range of 750–1080 cm^{-1} showed characteristic vibration bands at 1076, 945, 910, and 780 cm^{-1}. Corresponding to the vibrations of the polyoxoanion, the peak at 1076 cm^{-1} could be attributed to asymmetric stretch vibration of P–O_a (O_a = oxygen atom of tetrahedral phosphate). The asymmetric stretch vibration of Mo=O_t (O_t = terminal oxygen atoms) is observed at 945 cm^{-1}. The bending vibration of Mo–O_b–Mo (O_b = bridged oxygen of two tungsten atoms) and Mo–O_c–Mo (O_c = bridged oxygen at the corners of the Keggin structure) are observed at 910 and 780 cm^{-1}, respectively. In the FT-IR spectrum of PMoA (Figure 1b), the peaks observed at 1630 and 3438 cm^{-1} regions are related to OH bending and stretching vibrations in structure of pure $H_3PMo_{12}O_{40}$.

In the spectrum of the nanocatalyst (Figure 1a), almost all the peaks of neat $H_3PMo_{12}O_{40}$ (PMoA) are observed at 1077, 942, 906, and 789 cm^{-1}, indicating that polyoxoanion species is supported on G/MF@PANI. It has been reported that the interaction between the supported $H_3PMo_{12}O_{40}$ and PANI, in these types of composites, is attributed to chemical adsorption of polyoxoanion by PANI. In fact, the observed slight shifts of the FT-IR bands of the supported PMoA can be due to this interaction. The characteristic peaks at 1582 and 1490 cm^{-1} in the FT-IR spectrum of PANI are due to the presence of quinoid and benzenoid rings, respectively, in the polymer chain. Other observed peaks related to PANI match well with those reported in the literature for this conductive polymer.[37,38]

3.2 | PXRD analysis

The XRD patterns of G/MF and G/MF@PANI-PMoA compounds are presented in Figure 2. The expected peaks for $MnFe_2O_4$ are seen in the XRD patterns of both G/MF and G/MF@PANI-PMoA (Figure 2a,b). The diffraction peaks (2θ) of the $MnFe_2O_4$ at 30.1° (2 2 0), 35.2° (3 1 1), 43.0° (4 0 0), 53.1° (4 2 2), 56.6 (3 3 3), and 62.1° (4 4 0) are consistent with the standard PXRD data for the $MnFe_2O_4$ (JCPDS card, file no. 02-7158) with a face-centered cubic (fcc) structure. This observation confirms that the spinel cubic structure of the MF is retained in both of these samples. The intensity of the XRD peaks for G/MF@PANI-PMoA is somewhat lower than that of G/MF, which may be due to the interaction of the immobilized ionic liquid with MF nanoparticles. In addition to the MF peaks, other peaks are also seen in the XRD pattern of G/MF@PANI-PMoA, which can be ascribed to PMoA. The PXRD of G/MF@PANI-PMoA in Figure 2a shows the characteristic peaks of $MnFe_2O_4$, but the peaks are slightly shifted. The incorporation of PMoA into the MF lattice might be responsible for the larger lattice constants and d-spacing values. On the basis of Bragg's law, these shifts can be attributed to the change in the interplanar spacing in the framework structures. Also, in the XRD pattern of G/MF@PANI-PMoA nanocomposite, a broad peak was observed at 2θ less than 30°, which can be possibly due to the amorphous phases of graphene and/or PANI.[39,40]

3.3 | SEM and TEM analysis

The morphology of the as-synthesized nanocomposite was studied by SEM and TEM analysis. The SEM images of the synthesized nanocomposite are depicted in Figure 3. Graphene-like sheet structure coated with $MnFe_2O_4$ and functionalized with ionic liquid that are well integrated on the surface of graphene is clearly seen in Figure 3a,b. Its TEM images are presented in Figure 3c,d, which clearly shows spherical morphology with slight aggregation. The images indicate that ionic liquid attached to magnetic nanoparticles

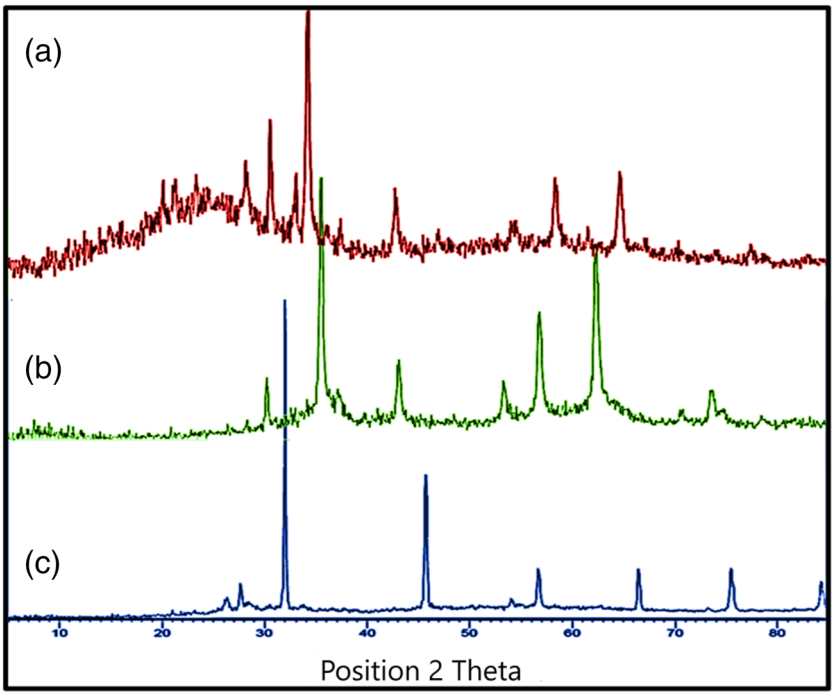

FIGURE 2 PXRD patterns of G/MF@PANI-PMoA (a), G/MF (b), and neat PMoA (c)

(seen as dark spots) is grafted on the graphene sheets (seen as bright sheets) with almost uniform distribution. A particle size distribution diagram and the selected area electron diffraction (SAED) of the G/MF@PANI-PMoA were shown in Figure 3e,f. The nanocomposite size distribution in Figure 3e shows an average particle size of 70–80 nm. It can be seen that the nanoparticles are fairly uniform in size. The six strong diffraction rings in the SAED were assigned to the (2 2 0), (3 1 1), (4 0 0), (4 2 2), (3 3 3), and (4 4 0) reflections of the cubic spinel structure of magnetite, respectively. This was in good agreement with the XRD results, indicating that $MnFe_2O_4$ particles have high crystallinity.

3.4 | Magnetic property

The magnetic property of G/MF@PANI-PMoA nanocomposite was measured at room temperature using the vibration sample magnetometer (VSM), and the magnetic hysteresis loops are shown in Figure 4. The value of saturation magnetization (Ms) for G/MF was 43.53 emu/g and decreased to 8.47 emu/g in the final G/MF@PANI-PMoA nanocomposite. The decrease of Ms can be attributed to the presence of nonmagnetic PANI and PMoA components on the surface of G/MF. In spite of the marked decrease of Ms, G/MF@PANI-PMoA composite still has significant magnetic property ensuring its effective recovery and separation from the reaction mixture by applying an external magnetic field.

3.5 | Thermal analysis

To characterize the thermal stabilities of synthesized magnetic nanocomposite, its thermal decomposition behavior was investigated by the TGA (Figure 5). The experiment was performed under nitrogen atmosphere at a heating rate of 10°C min^{-1} in the temperature range of 50–1000°C. On the basis of the TGA, Thermal decomposition of nanocomposites can be divided into two stages. The TGA curve showed a small weight loss (15%) starting at 50–317°C that can be attributed to the release of the water molecules and the first steps of degradation of PANI chains. A large weight loss of around 53% was observed at 545°C, which is related to the degradation of organic framework and also to the degradation of the $H_3PMo_{12}O_{40}$ molecules. The total weight of volatile material in the TGA curve for G/MF@PANI-PMoA is 68%.

3.6 | Evaluation of catalytic activity of G/MF@PANI-PMoA

In order to evaluate the catalytic activity of G/MF@PANI-PMoA nanocatalyst, it was examined as catalyst for the preparation of paracetamol and aspirin. The characterization of the produced paracetamol and aspirin samples was achieved by FT-IR, ^{1}HNMR, and CHN techniques. The FT-IR spectrum of paracetamol shows a peak at 1654 cm^{-1} related to the amide carbonyl stretching. Also, two peaks at 3327 and 3164 cm^{-1}

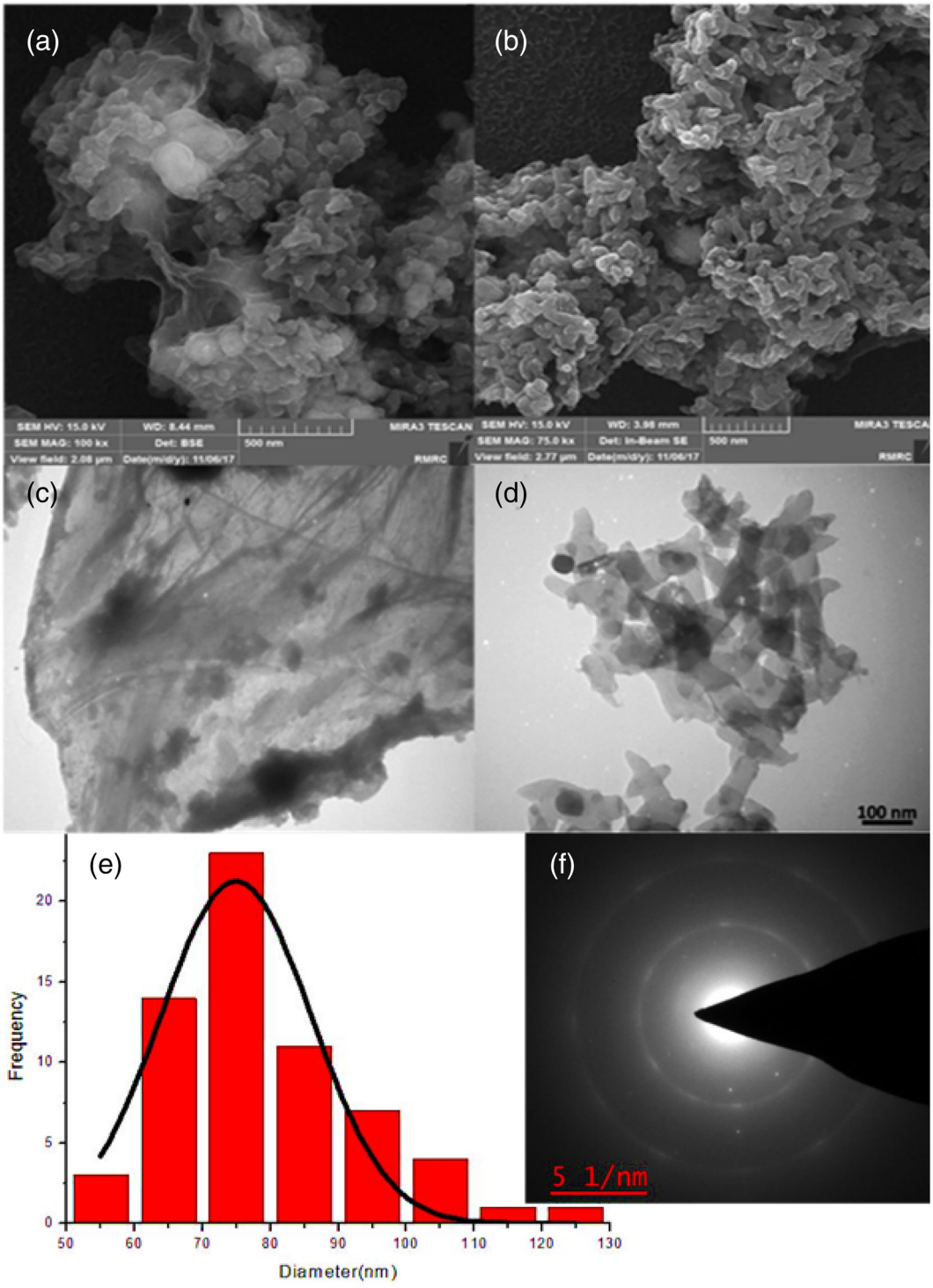

FIGURE 3 The FESEM images (a,b), TEM (c,d), particle size distribution diagram (e), and SAED of G/MF@PANI-PMoA (f)

are assigned to phenolic OH and N–H stretching, respectively (Figure S3). The synthesized paracetamol sample was further characterized by ^{1}H NMR spectroscopy using $CDCl_3$ as solvent. The methyl group protons were observed at 2.1 ppm. Aromatic protons of paracetamol appeared in the range of 6.5–7.5 ppm. The proton of the NH group was observed at 9.4 ppm and the proton of phenolic OH group at 10.2 ppm (Figure S4). The obtained results of CHN analysis for paracetamol: anal. calcd. for $C_8H_9NO_2$ C: 63.5, H:6.00, N: 9.26; found: C: 63.60, H:6.07, N: 9.35. Melting point: 170°C. The physical, ^{1}HNMR, and FT-IR spectral and CHN analysis data of the prepared paracetamol were compared with those reported in the literature.[41–44]

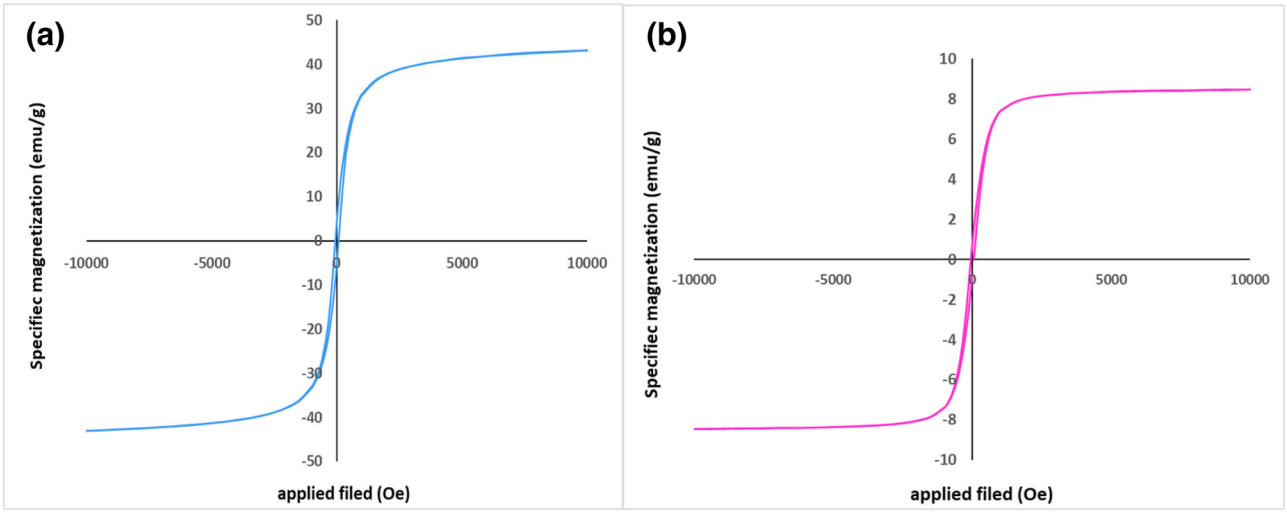

FIGURE 4 Hysteresis loops of G/MF (a) and G/MF@PANI-PMoA (b)

FIGURE 5 The TGA thermogram of G/MF@PANI-PMoA

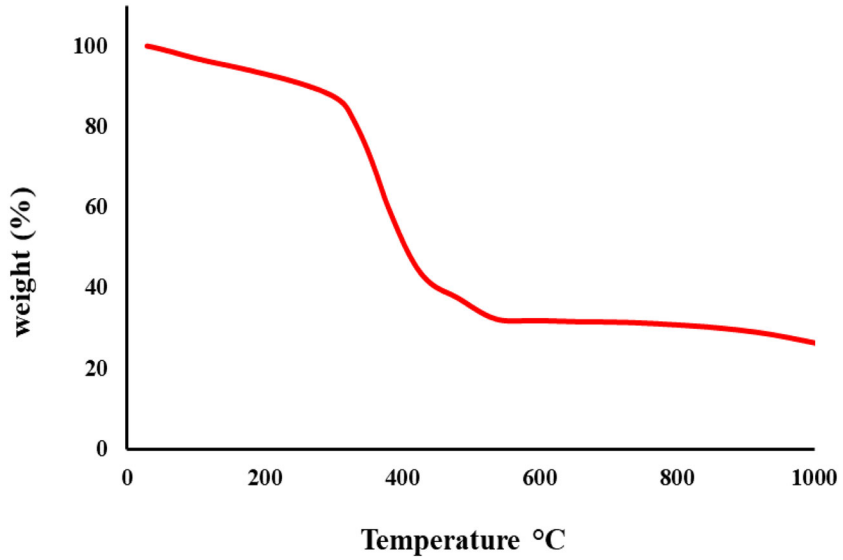

The newly made nanocatalyst was also used in the preparation of aspirin from salicylic acid and acetic anhydride. The FT-IR spectrum of the obtained aspirin from this catalytic system shows two peaks at 1741 and 1691 cm^{-1}, which are related to ester carbonyl and acidic carbonyl respectively (Figure S5). The structure of the synthesized aspirin was further confirmed by ^{1}H NMR study. The protons of methyl group in aspirin appeared at 2.37 ppm, aromatic protons in are observed in the range of 7.34–8.12 ppm, and the proton of the acidic OH group is seen at 10.91 ppm (Figure S6). The obtained results of CHN analysis: anal. calcd. for $C_9H_8O_4$ C: 60.00, H:4.47; found: C: 60.09, H:4.39. Melting point: 135°C. These results are in agreement with the other previously reported findings.[45–48]

The efficiency of the as-synthesized G/MF@PANI-PMoA heterogeneous nanocatalyst in preparation of paracetamol and aspirin can be attributed to the presence of PMoA, as Brønsted acid, in this nanocomposite. To further prove this idea, each of $MnFe_2O_4$, G/MF, and neat PMoA were examined separately for the preparation of paracetamol. As seen in Table 2, neither of $MnFe_2O_4$ or G/MF has shown any catalytic effect on this reaction; whereas PMoA was found to be nearly as effective catalyst as G/MF@PANI-PMoA. However, the difficulty in recovery and recycling of the pure PMoA limits its application as catalyst for these types of reactions.

3.7 | Recycling and reusing of the catalyst

Facile recovery is considered as valuable property for any heterogeneous catalytic system. In order to test the as-

TABLE 2 Stepwise optimization of catalyst for the synthesis of paracetamol

Entry	Catalysts[a]	Time (min)	Yield%
1	$MnFe_3O_4$	15	-
2	G/MF	15	-
3	$H_3PMo_{12}O_{40}$	15	85
4	G/MF@PANI-PMoA	15	73
5	G/MF@PANI-PMoA (0.1 g)	15	98

[a]Amount of catalyst: 0.05 g.

TABLE 3 Reusability of G/MF@PANI-PMoA

Run	Fresh	1	2	3	4
Yield (%) (paracetamol)	98	98	98	97	97
Yield (%) (aspirin)	97	97	96	97	96

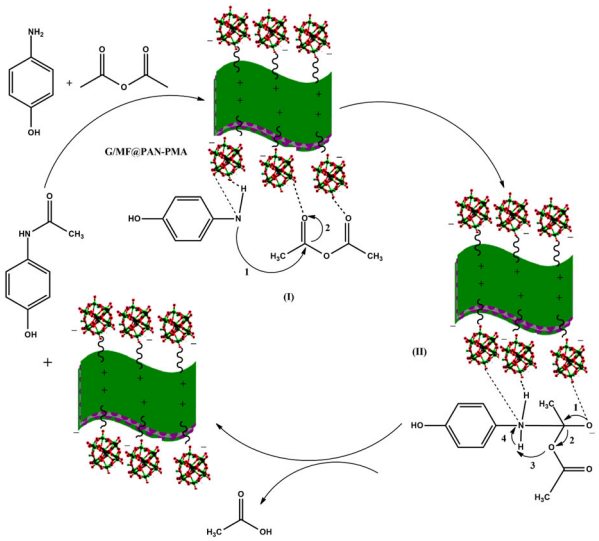

SCHEME 2 The proposed mechanism for the synthesis of paracetamol in the presence of G/MF@PANI-PMoA

fabricated catalyst reusability, aspirin and paracetamol preparation reactions were performed in the presence of catalytic amount of G/MF@PANI-PMoA under optimized reaction conditions. After completion of each reaction, the catalyst was isolated by applying an external magnetic force, followed by washing it for two times with ethanol. After drying the isolated catalyst, it was reused in a new reaction with fresh substrates. The reusability result of this catalyst is presented in Table 3, which indicates that the recovered catalyst could be reused for at least four successive times with almost the same catalytic activity. The amount of molybdenum was measured in the recycled nanocatalyst after four runs by ICP-AES analysis. This measurement showed that the molybdenum content of the recycled G/MF@PANI-PMoA, after four runs, was 0.356 mmol/g. This shows the loss of only 1.1% of the Mo amount in the original catalyst. This finding shows that leaching of the catalyst in this reaction is not significant, which indicates high stability of the present magnetic nanocatalyst. The FT-IR spectrum of the nanocatalyst after recovery is given in Figure S7 in which no clear change was observed after using the catalyst for four times. Furthermore, the TEM image of the nanocatalyst after recovery, presented in Figure S8, shows no clear change with the original sample, which also confirms the stability and green nature of the examined catalyst.

3.8 | Proposed mechanisms for preparation of paracetamol and aspirin

According to the previous studies and our experiences regarding these types of reactions, a tentative multistep mechanism can be proposed (see Scheme 2) for this catalytic system. In the preparation of paracetamol, first, the reaction starts with the adsorption process of the reactants to the surface of the catalyst, where the solitary pair of electrons in the carbonyl oxygen of the acetic anhydride and nitrogen and hydrogen of 4-hydroxyaniline are activated by interaction to ion liquid on surface of G/MF (Intermediate [I]). Then, the nitrogen of 4-hydroxyaniline, as nucleophilic group, attacks the carbon of acetic anhydride (electrophile) to form a protonated tetrahedral intermediate (Intermediate [II]). In the next step, the tetrahedral intermediate loses an acetic acid molecule and results in a protonated amide, which is still adsorbed to the catalyst surface. Thus, with the diffusion of acetic acid into the reaction medium, the desorption of the protonated amide is initiated with the transfer of electrons from catalyst to the oxygen of the carbonyl, thus breaking the bond and simultaneously the deprotonation of paracetamol and the regeneration of the catalyst.[9]

An analogous mechanism, as the one suggested for the paracetamol preparation, can be also proposed for the reaction of aspirin preparation (Scheme 3). Again, the starting precursors initially interact with ion liquid on surface of the nanocatalyst to give Intermediate (I). In the second step, the hydroxyl group of salicylic acid, as nucleophilic group, attacks the carbon of the carbonyl group of acetic anhydride to form Intermediate (II). The latter will then give Intermediate (III) through some rearrangement that finally passes through proton transfer and some other rearrangements ending to the formation of aspirin.[3]

SCHEME 3 Proposed mechanism for the preparation of aspirin in the presence of G/MF@PANI-PMoA

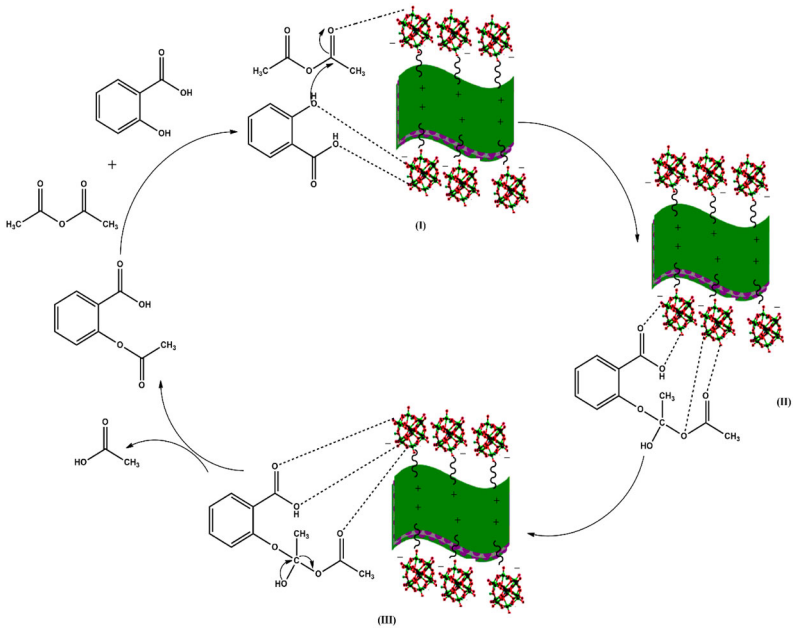

TABLE 4 Comparison of efficiency of the G/MF@PANI-PMoA in preparation of paracetamol with other catalysts

Entry	Catalyst	Solvent	Temp. °C	Time	Yield%	Ref.
1	EST-PtNP	-	RT	10 min	75	[8]
2	Ammonium acetate	-	220	15 h	95	[49]
3	Al-MCM-41/H_3PO_4	Acetone	70	1 h	81	[10]
4	Zeolite β or heteropolyacid	-	280–300	15 h	86	[50]
5	CF@[Cu_2(Si–N=SA)$_2$(2,2′-bipy)$_2$ (PTA)]	-	RT	1 min	98	[51]
6	G/MF@PANI-PMoA	-	RT	15 min	98	This work

3.9 | Comparison of the results of present work with previously reported works

In Tables 3 and 4, the catalytic activity of the as-prepared nanocatalyst was compared with other recently studied catalysts. Although some alternative catalysts have been so far introduced to improve the process of paracetamol and aspirin preparation, most of the used catalysts have their own limitations. One of the main encountered problems in using these catalysts is the difficulty of their regeneration and recycling for repeated usage in order to avoid releasing of hazardous waste into the environment. Harsh reaction condition is another drawback that most of the reported catalytic systems for these reactions are suffered from. The data in Table 4 show that the heterogeneous nanocatalyst of the present work is superior to the previously reported catalysts with respect to reaction times and reaction conditions.

Joncour et al. have recently designed a green chemical method for direct synthesis of paracetamol from hydroquinone reaction with high yield (95%). Unfortunately, this method has the limitations of high temperature (220°C) and long reaction time (15 h) (Table 4, Entry 2).[49]

Another method was used for the synthesis of paracetamol by Ghiaci and coworkers. In this reaction, an environmentally benign synthetic method using Al-MCM-41 modified with H_3PO_4 as solid acid catalyst presents some advantages; however, the use of solvent, the presence of H_3PO_4, and the low yield are considered as drawbacks of this system (Table 4, Entry 3).[10]

On the other hand, for the preparation of aspirin, two catalysts have been recently reported, which seem to be promising for improving the acetylation of salicylic acid. Tyagi et al.[4] have synthesized nanocrystalline sulfated zirconia solid acid catalyst, which was found to be efficient in minimal amount to give excellent yield of acetylsalicylic acid crystals from its precursors (Table 5, Entry 2). However, in spite of some advantages of this catalytic system, high yield of aspirin can be only obtained at reaction temperature of 120°C, and the molar

TABLE 5 Comparison of efficiency of the G/MF@PANI-PMoA in preparation of aspirin with other catalysts

Entry	Catalyst	Solvent	Temp. °C	Time(h)	Yield%	Ref.
1	WO_3/ZrO_2	-	120	2	80	[7]
2	Sulfated zirconia	-	90	2	95	[4]
3	$H_{14}[NaP_5W_{30}O_{110}]$	-	25	5	78	[2]
4	G/MF@PANI-PMoA	-	RT	30 min	97	This work

ratio of acetic anhydride to salicylic acid has to be higher than 3. In addition, the catalyst has to be heated at high temperature (450°C) for regeneration purposes. The other reported catalyst for this preparation is WO_3/ZrO_2 solid super-acid, which was designed by Zhang and coworkers. The synthesis of this catalyst, however, is rather tedious, and the obtained yield of acetylsalicylic acid using this catalyst was less than 80%. Also, the catalyst has to be calcined at 550°C before reuse in another reaction (Table 5, Entry 1).[7]

In brief, compared with the previous methods that had been used for the synthesis of paracetamol and aspirin, the current approach has advantages in terms of time, cost, and environmental safety. This is because the reactions were carried out at room temperature, solvent-free condition, and atmospheric pressure within a very short period of time, without using complex compounds or expensive equipment. Moreover, the advantage of our introduced nanocomposite will be more evident when its magnetic property is taken into account, which ensures facile and efficient separation of the nanocatalyst, one of the crucial steps in the recycling process. Consequently, according to all the advantages of the present catalytic system, it might be a potentially suitable method to be introduced for the preparation of paracetamol and aspirin drugs, as well as other similar organic compounds, at large scales.

4 | CONCLUSIONS

In the present work, we described a straightforward protocol for the synthesis of G/MF@PANI-PMoA, an ion liquid magnetic nanocomposite catalyst, containing a mineral acid. We also demonstrated that the prepared catalyst could be used for a one-pot preparation of paracetamol and aspirin drugs through a mild, fast, cost-effective, and environmentally friendly procedure. This method offers significant advantages compared with the currently available synthetic processes so far used for the synthesis of these important drugs. Therefore, the introduced nanocatalyst in this study may be practically used for large-scale production of various drugs in pharmaceutical industry.

ACKNOWLEDGMENTS

The authors wish to acknowledge the support of this work (Grant No. 1398) provided by the Research Council of Shahid Chamran University of Ahvaz, Iran.

DATA AVAILABILITY STATEMENT

The data that supports the findings of this study are available in the supplementary material of this article.

ORCID

Elahe Nasiri https://orcid.org/0000-0003-2701-4691
Feridoon Kooshki https://orcid.org/0000-0003-3079-3470
Mohammad Kooti https://orcid.org/0000-0002-5226-349X
Rezvan Rezaeinasab https://orcid.org/0000-0002-5638-3106

REFERENCES

[1] A. Majedi, F. Davar, A. Abbasi, *Ind. Eng. Chem.* **2014**, *20*, 4215.
[2] F. F. Bamoharram, M. M. Heravi, M. Roshani, A. Gharib, M. Jahangir, *J. Chin. Chem. Soc.* **2007**, *54*, 1017.
[3] D. Montes, M. Sanabria, J. Garcia, J. Castro, J. Fajardo, *J. Chem. Educ.* **2006**, *83*, 628.
[4] B. Tyagi, M. K. Mishral, R. V. Jasra, *J. Mol. Catal. A: Chem.* **2010**, *317*, 41.
[5] S. Jung, Y. Tsukuda, R. Kawashima, T. Ishiki, A. Matsumoto, A. Nakaniwa, M. Takagi, T. Noguchi, N. Imai, *Tetrahedron Lett.* **2013**, *54*, 5718.
[6] A. Bhattacharya, V. C. Purohit, V. Suarez, R. Tichkule, G. Parmer, F. Rinald, *Tetrahedron Lett.* **2006**, *47*, 1861.
[7] C. Zhang, T. Liu, H. J. Wang, F. Wang, X. Y. Pan, *Chem. Eng. J.* **2011**, *174*, 236.
[8] B. H. San, S. Ravichandran, K. Park, V. K. Subramani, K. K. Kim, *ACS Appl. Mater. Interfaces* **2016**, *8*, 30058.
[9] A. N. Oliveira, E. T. L. Lima, D. T. Oliveira, R. S. Angelica, E. H. A. Andrade, G. N. R. Filho, C. E. F. Costa, F. F. Costa, R. Luque, L. A. S. Nascimento, *Materials* **2019**, *12*, 2995.
[10] M. Ghiaci, H. Aghaei, M. Oroojeni, B. Aghabarari, V. Rives, M. A. Vicente, I. Sobrados, J. Sanz, *Catal. Commun.* **2009**, *10*, 1486.
[11] A. Shaabani, A. Maleki, *Appl. Catal. A: Gen.* **2007**, *331*, 149.
[12] Y. Leng, J. Zhao, P. Jiang, J. Wang, *ACS Appl. Mater. Interfaces* **2014**, *6*, 5947.
[13] W. R. K. Thalgaspitiya, T. K. Kapuge, J. He, P. Kerns, A. G. Meguerdichian, S. L. Suib, *Dalton Trans.* **2020**, *49*, 3786.

[14] M. Kooti, E. Nasiri, *J. Mol. Catal. A: Chem.* **2015**, *406*, 168.
[15] D. Zhang, D. Zhang, W. Zhang, Z. Lin, J. Dong, N. Zhen, Y. Chi, C. Hu, *Inorg. Chem.* **2020**, *59*, 9756.
[16] S. H. Mansourian, S. Shahhosseini, A. Maleki, *Russ. J. Appl. Chem.* **2019**, *92*, 1291.
[17] M. Lei, Q. Gao, K. Zhou, P. Gogoi, J. Liu, J. Wang, H. Song, S. Wang, X. Liu, *Sep. Purif. Technol.* **2021**, *257*, 117933.
[18] W. Xie, F. Wan, *Chem. Engin. J.* **2019**, *365*, 40.
[19] S. Saikia, R. Borah, *Appl. Organomet.* **2020**, *34*, 1.
[20] M. A. Rezvani, M. H. Seyed, A. Mirsadri, *Appl. Organomet.* **2020**, *34*, 1.
[21] L. Zhang, L. Zhang, M. Wana, *Eur. Polym. J.* **2008**, *44*, 2040.
[22] S. Zhang, P. He, W. Lei, G. Zhang, *J. Electroanal. Chem.* **2014**, *724*, 29.
[23] Z. Cui, C. X. Guo, C. M. Li, *J. Mater. Chem. A* **2013**, *1*, 6687.
[24] S. Ren, M. Xu, Y. Yang, S. Ma, C. Hao, *J. Appl. Polym. Sci.* **2014**, *131*, 41033.
[25] J. Gao, T. Yang, X. Wang, Q. He, P. He, L. Jia, L. Du, H. Deng, H. Zhang, B. Jia, X. He, B. Tang, *Microchem. J.* **2020**, *158*, 105158.
[26] P. R. A. Selvan, E. Subramanian, R. Murugesan, *J. Appl. Chem.* **2017**, *13*, 593.
[27] G. G. Papagianni, D. V. Stergiou, G. S. Armatas, M. G. Kanatzidis, M. I. Prodromidis, *Sens. Actuators B Chem.* **2012**, *173*, 346.
[28] L. C. P. Almeida, A. D. Gonçalves, J. E. Benedetti, P. C. M. L. Miranda, L. C. Passoni, A. F. Nogueira, *J. Mater. Sci.* **2010**, *45*, 5054.
[29] S. R. Thakare, V. R. Mate, K. Urkude, S. B. Gawande, *FlatChem* **2020**, *22*, 100179.
[30] R. G. Rani, S. Kumar, *Int. J. Hydrogen Energy* **2019**, *44*, 16933.
[31] A. Maleki, Z. Varzi, F. Hassanzadeh, *Polyhedron* **2019**, *171*, 193.
[32] A. Maleki, H. Movahed, P. Ravaghi, *Carbohydr. Polym.* **2017**, *156*, 259.
[33] A. Maleki, P. Zand, Z. Mohseni, *RSC Adv.* **2016**, *6*, 110928.
[34] A. Maleki, M. Azizi, Z. Emdadi, *Green Chem. Lett. Rev.* **2018**, *11*, 573.
[35] J. C. Bailar, H. S. Booth, M. Grennert, *Inorg. Synth.* **1939**, *1*, 132.
[36] M. Kooti, P. Kharazi, H. Motamedi, *J. Taiwan Inst. Chem. Eng.* **2014**, *45*, 2698.
[37] M. Ghorbanloo, H. Hosseini Monfared, C. Janiak, *J. Mol. Catal. A: Chem.* **2011**, *345*, 12.
[38] L. Lu, Y. Xie, *New J. Chem.* **2017**, *41*, 335.
[39] Z. Cui, C. X. Guoa, C. M. Li, *J. Mater. Chem. A, J. Mater. Chem. A* **2013**, *1*, 6687.
[40] J. Tao, *Appl. Mech. Mater.* **2014**, *484-485*, 137.
[41] M. L. Peterson, D. McIlroy, P. Shaw, J. P. Mustonen, M. Oliveira, O. Almarsson, *Cryst. Growth des.* **2003**, *3*, 761.
[42] M. A. Neumann, M. A. Perrin, *CrystEngComm* **2009**, *11*, 2475.
[43] V. K. Pecharsky, P. Y. Zavalij, *Fundamentals of Powder Diffraction and Structural Characterization of Materials*, Springer, Maryland, USA **2009**.
[44] M. A. Perrin, M. A. Neumann, H. Elmaleh, L. Zaske, *Chem. Commun.* **2009**, *14*, 3181.
[45] J. Olmsted III, *J. Chem. Educ.* **1998**, *75*, 1261.
[46] S. G. Zhang, *Fine Organic Chemicals Technique Handbook*, China Machine Press, Beijing, China **1991**.
[47] C. Ouvrard, S. L. Price, *Cryst. Growth des.* **2004**, *4*, 1119.
[48] X. Yan, H. He, J. Meng, C. Zhang, M. Hong, X. Tang, *Drug Dev. Ind. Pharm.* **2012**, *38*, 1221.
[49] R. Joncour, N. Duguet, E. Metay, A. Ferreira, M. Lemaire, *Green Chem.* **2014**, *16*, 2997.
[50] S. Gopinathan, C. Gopinathan, J. Kuruvilla, S. Pardhy, A. Ratnasamy, U.S. Patent 5856575, **1999**.
[51] M. Kooti, E. Nasiri, *Appl. Organomet. Chem.* **2018**, *32*, 1.

SUPPORTING INFORMATION

Additional supporting information may be found in the online version of the article at the publisher's website.

How to cite this article: E. Nasiri, F. Kooshki, M. Kooti, R. Rezaeinasab, *Appl Organomet Chem* **2021**, e6413. https://doi.org/10.1002/aoc.6413